

## Research Article

# Proteomics Characterization of the Secretome from Rat Pancreatic Stellate Cells with ATP-Binding Cassette Transporters (ABCG2) and NCAM Phenotype

**Maria Lucas,<sup>1</sup> Eugenia Mato,<sup>1,2</sup> Silvia Barceló-Batllori,<sup>1,3</sup> Ramon Gomis,<sup>1,4</sup> and Anna Novials<sup>1,4</sup>**

<sup>1</sup> Diabetes and Obesity Laboratory, August Pi i Sunyer Biomedical Research Institute (IDIBAPS), Endocrinology and Nutrition Unit-Hospital Clínic, Barcelona, Catalonia, Spain

<sup>2</sup> Biomedical Research Networking Centre on Bioengineering, Biomaterials & Nanomedicine: CIBER-BBN-EDUAB-HSP Group, Barcelona, Catalonia, Spain

<sup>3</sup> Proteomics Unit, Cancer Epigenetics and Biology Program (PEBC), Bellvitge Biomedical Research Institute (IDIBELL), Barcelona, Catalonia, Spain

<sup>4</sup> Spanish Biomedical Research Centre in Diabetes and Associated Metabolic Disorders (CIBERDEM), Barcelona, Catalonia, Spain

Correspondence should be addressed to Eugenia Mato; [emato@santpau.cat](mailto:emato@santpau.cat) and Anna Novials; [anovials@clinic.ub.es](mailto:anovials@clinic.ub.es)

Received 1 July 2013; Accepted 4 August 2013

Academic Editors: A. Hergovich and A. A. Minin

Copyright © 2013 Maria Lucas et al. This is an open access article distributed under the Creative Commons Attribution License, which permits unrestricted use, distribution, and reproduction in any medium, provided the original work is properly cited.

We have previously reported the identification of a pancreata mitoxantrone-resistant cell population which expressed the ABCG2 transporter with a pancreatic stellate cells phenotype (PaSC) and ability of secreting insulin after inducing their differentiation. The characterization of the secretome of this cell population by two-dimensional electrophoresis (2D) coupled with mass spectrometry MALDI-TOF was able to identify seventy-six protein spots involved in different cellular processes: development/differentiation, proteases, immune response, and other. Moreover, Ingenuity Pathway Analysis displayed several significant networks and TGF $\beta$ 1 molecule was identified as a central node of one of them. The effect of this active molecule secreted in the conditioned medium was investigated in ductal cell line (ARIP). The results showed that the conditioned medium inhibited their proliferation without affecting their cell viability. Additionally, they showed an upregulation of PDX1 and downregulation of CK19. The rate of ARIP cell proliferation was recovered, but no effects on the gene expression were observed after using TGF $\beta$ 1-neutralising antibody. Proteins associated with cell growth, development and differentiation such as PEDF, LIF, and Wnt5b, identified in the secretome, could be involved in the observed transcription changes. These finding may suggest a new paracrine action of PaSCs involved in the proliferation and differentiation pathways not yet identified.

## 1. Introduction

Pancreatic stellate cells (PaSC) were first described in 1998 and constitute nearly 4% of total pancreatic cells [1]. PaSCs are located in the periacinar space and can also be found in the periductal regions of the pancreas [2]. These cells have long cytoplasmic processes resulting in a typical “stellate” appearance. They share morphological and functional characteristics with the hepatic stellate cells and can present different phenotypes: quiescent cells, with capacity to storage vitamin A, and active cells, also so-called myofibroblast-like

cells. The active phenotype expresses alpha actin ( $\alpha$ SMA), desmin, glial fibrillary acidic protein (GFAP), ABCG2, and NCAM. These latter two markers are expressed in rat and human hepatic stellate cells, and several studies demonstrate that NCAM is involved in the transformation of these cells in myofibroblasts and modulates the adhesive property of cell adhesion [3], and ABCG2 transporter is associated with cell viability and/or activation [4]. They can be useful to select PaSC with a myofibroblast phenotype. Moreover, several studies demonstrated that the soluble factors secreted by PaSCs with active phenotype, which are increased in areas

of pancreatic injury, play an important role in pancreas physiology, development of pancreatic fibrosis [5], antigen presentation, phagocytosis phenomena [6], and matrix turnover processes [7].

It is known that endocrine pancreatic tissue is able to regenerate in several species of mammals, including humans. Several studies support the hypothesis that this islet neogenesis in the mature pancreas occurs via cells which are located in or which are associated with the ductal epithelium. Ductal cells have the capacity to transdifferentiate into insulin producing cells, both in animal models and humans [8–11]. The role of surrounding cells may be important in maintaining their cellular niche, giving them the necessary factors to start the transdifferentiation process. Considering that PaSCs are also present in the same niche as ductal cells, for instance, periacinar and periductal regions, it is likely that PaSC secreted factors could have effects on neighbouring cells, as well as on the putative pancreatic progenitors.

The present study was designed to characterize the secretome of mitoxantrone-resistant cells obtained from lactating rats pancreata expressing the ABCG2 transporter and NCAM markers, with a PaSC phenotype (PaSCs-ABCG2(+)) and ability to secrete insulin after differentiation [12].

## 2. Materials and Methods

**2.1. Primary Cell Culture of Mitoxantrone-Resistant Cells Expressing Active Pancreatic Stellate Cells Phenotype Obtained by Drug Selection and Enriched by PSA-NCAM Immunopanning Technique.** All animal experimental proceeds were approved by the Institutional Animal Care and Use Committee of the IDIBAPS Research Institute, Barcelona, Spain. Fresh pancreata were removed from lactating rats and digested with collagenase to obtain a primary cell culture. This culture was grown in Dulbecco's Modified Eagle Medium (DMEM) (Gibco-BRL, Gaithersburg, MD, USA) (25 mM of glucose) supplemented with 10% fetal calf serum (FCS), and 100 U/mL of penicillin and mitoxantrone drug at 8  $\mu$ M (Sigma-Aldrich St. Louis, MO, USA) was added to the medium. This drug acts through multidrug transporter systems and permits the selection of cells which express the ABCG2 transporter, as described by Mato et al. [12]. The culture was maintained at 37°C in a humidified atmosphere containing 5% CO<sub>2</sub> and was expanded and the active pancreatic stellate cell phenotype was checked by immunocharacterization (alpha-actin, vimentin, desmin, chromogranin A, GFAP, and NCAM), RT-PCR expression (ABCG2), or oil-red staining as described by Mato et al. [12]. It is known that in mammals, PSA-NCAM is involved in the development of the nervous system and in tissue remodeling [13] and it also can induce proliferation in activated pancreatic stellate cells. In order to enrich active stellate cells fraction in our primary culture, we performed immunopanning as previously described by Ben-Hur et al. [14] using the sialylated-neural adhesion molecule isoform of NCAM (PSA-NCAM). Petridishes (Falcon Optilux) were first coated with secondary antibody IgM (Sigma-Aldrich) at 1:128 in 50 mM Tris-HCl buffer, pH 9.5, for 18 hours at 4°C. The plates were then washed three times in PBS and coated with anti-PSA-NCAM

antibody (USBiological, Swampscott, MA, USA) at 1:250 dilution in PBS with 0.2% BSA at room temperature for at least 1 hour. Cells were plated at  $1 \times 10^6$  cells/100 mm dish coated for PSA-immunopanning and were allowed to bind at 37°C for 30 minutes. Nonadherent cells, so-called negative fraction, were washed off extensively to discard them. The adherent cells corresponded to the positive fraction that expressed that PSA-NCAM were trypsinised, washed three times, and resuspended in fresh DMEM-F12, and a second PSA-NCAM immunopanning was redone. Before using the positive fraction of the cell in different experiments, the pancreatic stellate cell phenotype was confirmed by immunocytochemistry and flow cytometry each time. After the second immunopanning (positive PSA-NCAM fraction) conditioned media from active PaSCs-ABCG2(+) were collected every 48 hours and frozen at -80°C until used for subsequent analysis. For proteome analysis, conditioned media were collected as described: active PaSCs-ABCG2(+) cells were washed 3 times in PBS and cultured in serum-free media for 24 hours. This media was collected and centrifuged at 5000 g for 10 minutes to remove cell debris, after which the supernatant was frozen at -80°C until use.

**2.2. Flow Cytometry.** One million PBS-washed cells were resuspended in 875  $\mu$ L of cold PBS. Then, 125  $\mu$ L of cold 2% formaldehyde solution was added and the mixture was immediately vortexed for a brief period. The suspension was incubated for 1 hour at 4°C and centrifuged for 5 minutes at 250 g, after which the supernatant was removed. The pellet was gently resuspended in 1 mL of cold blocking solution (0.2% BSA in PBS), and the mixture was incubated for 1 hour at 4°C. One mL of buffer was added and the suspension was spun down for 5 minutes at 250 g. The supernatant was removed, and 50  $\mu$ L of primary antibody PSA-NCAM (USBiological) was added at a dilution 1:10 in blocking solution. The sample was incubated overnight at 4°C in the dark, washed twice with 1 mL of PBS by centrifugation at 250 g for 5 minutes, and resuspended in 500  $\mu$ L of secondary antibody (IgM, Sigma-Aldrich) at a dilution 1:128 in blocking solution. After 1 hour of incubation at 4°C, samples were washed twice with 1 mL of PBS by centrifugation at 250 g for 5 minutes and resuspended in 500  $\mu$ L of PBS. The labelled cells were analysed on a FACS Calibur (BD, San Jose, CA, USA) by acquisition of 10,000 gated events. Data was stored as listmode files and analysed with CellQuest (BD) and Summit Workstation software.

**2.3. ARIP Cell Culture and Treatment.** ARIP cell line were obtained from ATCC (CRL-1674 clon) and cultured in ARIP media: DMEM 24 mM glucose plus glutamine, nonessential amino acids, 100 U/mL of penicillin, and 10% FCS. Cells were treated with PaSC conditioned media for 24 or 72 hours. DMEM/F12 (8 mM glucose) supplemented with 10% FCS (PaSCs ABCG2(+) media) were used as basal media. All the experiments were performed using low passages from 16 to 19 of the cell culture.

**2.4. Proliferation and Viability Assays.** ARIP cells were seeded in 96-well tissue culture plates at a density of 50,000 cells/well

and incubated for 24 hours until adherence. Cells were then incubated in serum-free DMEM overnight and exposed to 15% FCS for 24 hours. Cells were either treated with pan TGF $\beta$  20  $\mu$ g/mL (R&D Systems, Minneapolis, MN, USA), TGF $\beta$ 1 10 ng/mL (R&D Systems), or nonimmune IgG 20  $\mu$ g/mL (Dako, Glostrup, Denmark), with the final 4 hours in the presence of 10  $\mu$ M BrdU. BrdU incorporation into ARIP cell DNA was assessed by measuring the absorbance at 450 nm, following cell proliferation ELISA kits instructions (Roche, Penzberg, Germany).

To conduct the viability assays, ARIP cells were seeded in 96-well tissue culture plates at a density of 50,000 cells/well and incubated for 24 hours until adherence. Cells were then incubated in serum-free DMEM overnight and exposed to 15% FCS for 24 hours, with the final 2 hours in the presence of 0.5 mg/mL MTT (Sigma-Aldrich, St. Louis, Missouri). Finally, 115  $\mu$ L of isopropanol plus 0.04 N HCl was added, samples were mixed well to dissolve crystals, and absorbance was measured at 575 nm.

**2.5. RT-PCR.** Total RNA was extracted from ARIP cultures using TRIzol reagent (Invitrogen, Carlsbad, CA, USA). To remove genomic DNA contamination, samples were treated with DNase I (Invitrogen), following the manufacturer's instructions. In addition, DNA-PCR without RT was included as a control. One  $\mu$ g of total RNA was reverse transcribed in a buffer solution containing 25 nmol/L MgCl<sub>2</sub>, 100 mmol/L Tris (pH 8.3), 500 mmol/L KCl, RNAGuard 39 U/mL (Pharmacia, Uppsala, Sweden), M-MLV-RT 200 U/mL (Gibco, Uxbridge, UK), 10 mmol/L deoxynucleotide triphosphate(s), and random hexamer priming d(N6)5'PO4 (Pharmacia). Complementary DNA (cDNA) was stored at -80°C until use. All PCRs were performed using 35 cycles. PCR products were visualised with 1% agarose gel electrophoresis and ethidium bromide staining.

**2.6. Real-Time PCR.** Real-time PCR was performed using the double stranded DNA binding dye Power SYBR Green PCR Master Mix using the ABI Prism 7900HT Sequence Detection System (Applied Biosystems, Foster City, California, USA). The sequences of primers used in this study are described in Table 1. A standard curve was generated from five serial dilutions of ARIP cDNA for CK19 and INS1E cDNA for PDX1. Samples were analysed in triplicate, negative controls were included, and PCR products were verified using dissociation curve analysis immediately after RT-PCR. Expressions of all target genes were determined by normalising the respective TATA Binding Protein (TBP) levels as a housekeeping gene. Results were analysed using SDS2.1 software (Applied Biosystems).

The oligonucleotide sequences used for PCR and real-time PCR amplification are summarised in Table 1.

**2.7. Immunocharacterization of PDX1 and CK19.** ARIP cells were plated in 8-well chamber slides (LAB-TEK, Campbell, CA, USA). After treatment with control or conditioned media for 72 hours, cells were fixed in 4% paraformaldehyde. They were then blocked for 10 minutes at room temperature in

1% BSA and then permeabilized with buffer containing 1% BSA and 0.2% saponin for 30 minutes at room temperature. Primary antibodies (PDX1-1:100, Santa Cruz, Santa Cruz, CA, USA; CK19-1:500, Dako) were diluted in fresh blocking solution, and the slides were then incubated overnight at 4°C following standard protocols. The reaction was visualised with a fluorescent secondary antibody (1:1000) under a Leica fluorescence microscope. 1% BSA was used instead of primary antibodies for control slides.

**2.8. Characterisation of the Secreted Proteins from the Active PaSC-ABCG2(+) Conditioned Media.** Conditioned media and serum-free conditioned media were collected as described before. Culture media alone (basal) were used as a blank and were also incubated without cells during 24 hours and collected. Centricon Amicon (Millipore, MA, USA) centrifugal filters with a 10 kDa molecular weight cutoff were used to concentrate conditioned media from 10 mL to 200  $\mu$ L, following the manufacturer's instructions. Proteins were precipitated using the 2D Clean Up Kit (GE Healthcare, United Kingdom) and were resuspended in a solution containing Tris (30 mM), urea (7 M), thiourea (2 M), and CHAPS (4%) compatible with first dimension isoelectric focusing (IEF). Protein content was quantified using the RC DC protein assay kit (BioRad, Hercules, CA, USA) based on the Lowry assay.

Protein extracts (100  $\mu$ g) were separated using IPG strips of pH 3–10 (17 cm, BioRad). Two-dimensional electrophoresis was carried out [15]. Briefly, isoelectric focusing was performed in Protean IEF Cell (Biorad) at 62 kVh and second dimension SDS-PAGE were run by overlaying the strips on 12% acrylamide home-made gels. Proteins were visualised using a MS compatible silver stain [16]. Gels were calibrated using MW and pI standards (Biorad). Differential expression of proteins from blank, conditioned media and serum-free conditioned media were analysed using Melanie-III software (BioRad). First, conditioned media and serum-free conditioned media were compared to ensure that serum was not affecting the secretome pattern. Proteins present in the conditioned media (both serum and serum-free), but absent in blank media, were considered as PaSC secreted. Secreted proteins were excised from serum-free conditioned media gels ( $n = 5$ ), silver destained and in-gel digested with trypsin (Promega, Madison, WI, USA) 37°C overnight. Peptide extraction was performed and Zip-Tip concentrating and desalting was done [17]. Peptides were analysed by MALDI-TOF MS and proteins were identified by peptide mass fingerprinting [18].

**2.9. Amino Acid Sequence Search for Features of Secreted Proteins.** The amino acid sequence of the identified proteins was analysed with SecretomeP 2.0 Server. SignalP 3.0, which predicts the presence and location of signal peptide cleavage sites in the N-terminal part (first 70 residues), identified proteins secreted via the classical pathway [19]. If no signal peptide was predicted, but the Neural Network score exceeded a value of 0.5, proteins were classified as secreted via the nonclassical pathways. SignalP 3.0 has been used to identify secreted proteins in other secretome studies [20, 21].

TABLE 1: List of all the primers used in this study.

Name	Sequence	bp	F/R	T annealing	GenBank accession numbers
Calreticulin	GGGCCCCTGATACCAAATGTC CTCTCGCCGCTGCCTTCC	467	FW RV	57°C	XM_001067664
Wnt5b	GCGCTGCTGGTGTGGTGAATG CCGGGCTGGGCTGGTTGA	415	FW RV	60°C	XM_342747
Calumenin	AGCTCCGGGGAAAACACTCAG CTCCGCTCATCTCTAACCATAATC	501	FW RV	60°C	NM_022535
SPARC	AAACCCCTGCCAGAACCATCATTG CTCCAGGCGCTTCTCGTTCTCGTG	415	FW RV	60°C	NM_012656
DIXDC1	GGGCAAATATGGATAAAGGATGAGC GTGACCGCCCCGAACC	435	FW RV	57°C	NM_001037654
Neuromodulin (GAP 43)	CTCCCCTTGCTGATGGTGTGG GGTCAGCCTCGGGTCTTCTTTAC	453	FW RV	60.5°C	NM_017195
Synaptotagmin V	CAGGGCAGAACACGCACGCACATA CTCCGGCCCAGTCTCTTCACTTCC	524	FW RV	59°C	BC_092198
Transcobalamin 2	TGGGCCAGCGTCTCTTACCTT CCGGCCATGGCTTCTGTGTC	508	FW RV	60.5°C	NM_022534
PEDF (serpin F1)	GGAGCCCGTAGTGGAGGAGGATGA ATGCGAGGGTTGCCAGTGAGGATT	417	FW RV	60°C	BC_078686
AHNAK	GTCGGTCTCTCAAGTCTCCATAACC TCCCCGACACTTTCACACCATCT	482	FW RV	57°C	XR_005457
DHRS4	AGGCGGCTCGGTGGTGATT TGGCGGTGGCAAGGAAGG	441	FW RV	58°C	NM_153315
Glypican 1 variant	GCTGCTGCTGCCGATGACTAT CCGCAGCCCTGGATGACCTTA	489	FW RV	61°C	NM_030828
RAB15	GCCGGGCCGCTTCCTTCT GCGCTCGCTGCTAATGTCGTA	404	FW RV	61°C	NM_198749
ARHGEF2	AGACCCGGGAAAAGGAGAAGATGA TGACGCAGCCCCAGAGGAGAC	445	FW RV	58°C	NM_001012079
Islet cell autoantigen 1-like	TCGGTTTGCTCAAGATAAGTCAGT TGGCCCGATGTCTAAAAGTCTCTA	404	FW RV	54.5°C	NM_030844
Leukemia inhibitory factor	AGGTCTTGCCGCAGGGATTG TCGGGGACACAGGGCACAT	508	FW RV	58°C	NM_022196
ERABP	CATGGTGGTCGAGCTGAAAGAGAA GTAGGGAAGGAGAGGCCAGGTAGG	448	FW RV	55°C	NM_024136
RAB14	TCGGGGATATGGGAGTAGGAA GGGGCTGAGGGTTTGTGTTGTA	541	FW RV	54.5°C	NM_053589
APG16 autophagy 16-like	CGGCCACAGCGGGAAAGTT CCCACGCCACCGCATTGATAGAAG	542	FW RV	58°C	XM_001067061
MMP2	GCTGATACTGACACTGGTACTG CAATCTTTTCTGGGAGCTC	217	FW RV	60°C	NM_031054
Collagen I	GCCACCTCAAGAGAAGTC ATAGCGACATCGGCAGGATCG	440	FW RV	58.5°C	BC133728.1
Vimentin	GCCAGCAGTATGAAAAGTGTG AGTGGGTGTCAACCAGAGGAA	496	FW RV	60°C	NM_031140
Desmin	AGACTTGACTCAGGCAGCCAAT CGGAAGTTGAGAGCAGAGAAGG	384	FW RV	60°C	NM_022531
GFAP	TGGCCACCAGTAACATGCA GACTCCTTAATGACCTCGCCAT	538	FW RV	60°C	NM_017009
TBP	ACCCTTCACCAATGACTCCTATG ATGATGACTGCAGCAAATCGC	190	FW RV	60°C	NM_001004198
PDX1	GAGCCAGCCGCTTCATCT CCCCGCTCGTTGTCCCCTACTA	318	FW RV	60°C	NM_022852

TABLE 1: Continued.

Name	Sequence	bp	F/R	T annealing	GenBank accession numbers
CK19	ACAGCCAGTACTTCAAGACC CTGTGTCAGCACGCACGTTA	690	FW RV	57°C	AY_464140
RTGFB I	ACCGCGTGCCAAATGAAGAGGAT TGCCGTGGACAGAGCGAGTTTGAT	464	FW RV	55°C	L26110.1
RTGFB II	TGGCCGCTGCACATCGTCCTG CTCGCCCGCCCTTTTCTTTTCCTT	366	FW RV	55°C	AF474028.1
RTGFB III	AGCAGCGCGGCCACAGCATC GAAGGGGGCATCCAGGGCGAGACT	531	FW RV	55°C	NM_017256.1
TBP real time	TTCGTGCCAGAAATGCTGAA GTTTCGTGGCTCTCTATTCTCATG		FW RV		NM_001004198
PDX1 real time	CCGCGTTCATCTCCCTTTC CTCCTGCCCACTGGCTTTT		FW RV		NM_022852
CK19 real time	AAGGTCAGGACCTTGAGATTG		FW		AY_464140

**2.10. Detection of TGF $\beta$ 1 in the Conditioned Media.** For TGF $\beta$ 1 detection, conditioned media were collected as for proteome analysis. One hundred  $\mu$ L/well of the capture antibody (R&D Systems, Minneapolis, MN, USA) diluted 2  $\mu$ g/mL in PBS was transferred to an ELISA plate and incubated overnight at room temperature. Five separate washing were performed. In the first washing of three times with PBS 0.05% Tween 20, the plate was blocked with PBS containing 5% Tween 20 and 5% sucrose for 1 hour. In the second washing of three times with PBS 0.05% Tween 20, 100  $\mu$ L of samples (conditioned media) and dilutions of standards of recombinant human TGF $\beta$ 1 (R&D Systems) were added and incubated for 2 hours at room temperature. In the third washing of three times with PBS 0.05% Tween 20, 100  $\mu$ L of detection antibody biotinylated anti-TGF $\beta$ 1 (R&D Systems) at 400 ng/mL was added and incubated 2 hours at room temperature. In the fourth washing of three times with PBS 0.05% Tween 20, 100  $\mu$ L of streptavidin HRP was added for 20 minutes at room temperature. In the final washing of three times with PBS 0.05% Tween 20, 100  $\mu$ L of substrate solution was added for 30 minutes, avoiding placing the plate in direct light. 50  $\mu$ L of 1 M H<sub>2</sub>SO<sub>4</sub> was added to each well and absorbance was measured at 450 nm.

**2.11. Statistical Analysis.** Results are expressed as mean  $\pm$  SEM; *n* represents the number of individual PaSC-ABCG2+ preparations. The statistical significance of the differences between groups was estimated using Student's unpaired *t*-test; \* indicate statistical significance with *P* < 0.05.

### 3. Results

**3.1. Immunopanning PSA-NCAM Enrichment from PaSC-ABCG2(+) Primary Culture.** Flow cytometry PSA-NCAM analysis of mitoxantrone-resistant cells maintained in the basal cell culture condition described before showed a 36% of positivity for this marker. In order to conduct the secretome analysis, we enriched the cell population for polysialylated isoforms of the neural cell adhesion molecule (PSA-NCAM)

by immunopanning technique, showing an increase of 57% of PSA-NCAM positivity in the first immunopanning up to 80% when the second immunopanning was redone. Then we confirm the active pancreatic stellate phenotype by immunocharacterization and ABCG2 expression each time (data not shown).

**3.2. Secretome Analysis of PaSC-ABCG2(+).** Conditioned media were prepared from active PaSC-ABCG2(+) cultured in serum-free conditions and subjected to 2-dimensional gel electrophoresis and silver staining. A preliminary study showed no differences in the secretion pattern between conditioned media and serum-free conditioned media. We decided to use serum-free conditioned media in order to eliminate serum-derived proteins from the media and to potentiate the less abundant proteins secreted from this cell population. The conditioned media 2D gels displayed a mean of 112 protein spots, which were selected for trypsin digestion and mass spectrometry MALDI-TOF analysis, and 76 spots were identified. Figure 1(a) is a representative image showing a 2D gel from PaSC-ABCG2(+) conditioned media with all the proteins identified. The majority of spots contained only single proteins, but in some cases MS analyses indicated a protein mixture. On the other hand, multiple spots flagged the same protein identity, thus suggesting posttranslational modifications or different isoforms. Overall, 61 different proteins were identified in the PaSC-ABCG2(+) secretome. Proteins along with Swiss-Prot accession number, annotations regarding prediction of secretion, and information related to peptide mass fingerprinting identification are listed in Table 2. Functional categories of the identified protein were proteolysis and related proteins, structural and cytoskeleton proteins, associated with cell growth, development, and differentiation, chaperones, metabolism, transport proteins, GTPase-related proteins, immune response, extracellular matrix and related proteins, and retinol related proteins. The identified proteins were analysed with SignalP V3 software which has been used to predict potential protein secretion [20, 21]. Sixty-one percent of the proteins were predicted to

TABLE 2: List of the proteins obtained in the secretome of PaSCs-ABCG2(+).

Protein number	Protein name	UniProt ID	pI (T)	MW (T)	pI (E)	MW (E)	n.pep	% Cov	Secretion
Proteolysis and related proteins									
1	Procollagen C-endopeptidase enhancer 1	O08628	8,2	48000	7,1	55793	8	18	1
1	Procollagen C-endopeptidase enhancer 1	O08628	8,2	48000	7,6	55793	7	18	1
1	Procollagen C-endopeptidase enhancer 1	O08628	8,2	48000	6,7	56509	11	33	1
1	Procollagen C-endopeptidase enhancer 1	O08628	8,2	48000	6,2	57108	10	28	1
2	72 kDa type IV collagenase (MMP2)	P33436	5,1	62000	5,0	68834	16	26	1
3	Alpha-2 antiplasmin	Q80ZA3	6	46000	5,5	52395	10	28	1
3	Alpha-2 antiplasmin	Q80ZA3	6	46000	5,4	53373	9	26	1
4	Isoform 4 of ubiquitin carboxyl-terminal hydrolase 15	Q8R5H1-4	5,4	26000	5,3	31776	8	38	2
5	Adult male cDNA proteasome regulatory particle	Q8CIT2	4,9	28000	4,9	31776	5	22	3
6	Cathepsin B.	Q6IN22	5,5	38000	5,1	42629	6	23	1
7	ATPase 3 (Fragment)	Q6PW16	6,2	14000	7,1	27988	7	57	2
Structural and cytoskeleton proteins									
8	Glial fibrillary acidic protein (fragment)	Q866S9	5,2	48000	4,7	44342	11	24	2
8	Glial fibrillary acidic protein (fragment)	P03995	5,4	50000	5,0	31776	9	21	2
9	Testis cDNA, similar to human desmin	Q4R7K6	5,1	24000	4,7	24070	12	38	2
10	Vimentin	P31000	5,1	54000	4,5	23085	15	22	2
10	Vimentin	P31000	5,1	54000	5,1	22777	14	23	2
10	Vimentin	P31000	5,1	54000	4,6	21138	17	28	2
10	Vimentin	P31000	5,1	54000	4,6	20825	13	22	2
11	Tropomyosin-1	Q60527	4,6	33000	4,6	40365	16	51	3
11	Tropomyosin alpha isoform	Q923Z2	4,7	33000	4,6	36876	8	24	3
11	Tropomyosin isoform 8 of P04692	P04692-8	4,8	29000	4,9	37590	7	24	3
11	Tropomyosin isoform 4 of P04692	P04692-4	4,8	29000	5,4	42564	10	38	3
12	Alpha-tropomyosin 3	Q63607	4,7	33000	9,3	49605	11	29	2
13	Tropomyosin 3, gamma	Q8K0Z5	4,7	33000	4,8	27739	10	32	3
14	Tropomyosin isoform 6	Q63610	4,8	29000	4,7	32061	14	46	3
14	Tropomyosin isoform 6	Q63610	4,8	29000	4,8	32157	8	36	3
15	Tropomyosin alpha-4 chain	P09495	4,7	28000	4,6	32471	15	43	3
16	Lamin-A	P48679	6,5	74000	5,2	42694	13	21	3
16	LMNA protein	Q8N519	6	53000	5,5	38527	10	19	3
17	Lamin-B2	P21619	5,4	67000	5,6	59799	12	18	3
18	Transgelin.	P31232	8,9	22000	9,6	24360	7	40	2
19	Myosin light polypeptide 6	Q64119	4,5	17000	4,3	19735	5	39	1
Associated with cell growth, development, and differentiation									
20	Neuromodulin	Q6S9D9	4,7	25000	4,5	23714	9	22	3
21	Pigment epithelium-derived factor	P97298	6,5	44000	5,5	52395	8	20	1
21	Pigment epithelium-derived factor	P97298	6,5	44000	5,4	51521	6	14	1
22	Protein Wnt-5b	Q9HIJ7	8,8	39000	5,7	23432	8	20	1
23	DIXDC1 protein (fragment)	Q8IVY4	6	41000	6,0	33333	9	24	3
24	AHNAK1 (fragment)	Q38PG1	5,2	59000	5,2	38623	14	22	3
25	SPARC	Q6GSZ4	4,8	34000	4,7	44342	15	38	1
26	Leukemia inhibitory factor	PI7777	9	20000	6,0	23432	4	30	1
Chaperones									
27	Calreticulin	P18418	4,3	46000	4,3	53430	14	38	1
28	Heat shock protein 8	Q4FZY7	5,4	71000	5,4	69248	26	51	3

TABLE 2: Continued.

Protein number	Protein name	UniProt ID	pI (T)	MW (T)	pI (E)	MW (E)	n.pep	% Cov	Secretion
29	78 kDa glucose-regulated protein	P06761	5	70000	5,0	68834	13	25	1
30	Serpinh1 protein	Q5RJR9	8,9	47000	9,3	49605	17	40	1
31	Calumenin	O35783	4,4	35000	4,3	49231	5	24	1
Metabolism									
32	Phosphoglycerate kinase 1	P16617	7,5	44000	8,0	46687	14	41	3
33	Enolase 1, alpha	Q5EB49	6,2	47000	6,0	53471	10	28	2
34	Fructose-bisphosphate aldolase A	P05065	8,4	39000	8,8	42888	12	29	3
35	Isoform M2 of Pyruvate kinase	P11980-2	7,4	58000	7,4	61394	23	52	3
36	Carbonyl reductase [NADPH] 1	P47727	8,2	30000	6,7	27573	9	32	2
37	Adult male cDNA, similar to GTPasa	Q3UH20	7	43000	4,6	28837	12	20	3
Transport proteins									
38	Transcobalamin-2	Q9R0D6	7,8	46000	8,0	46687	11	25	1
39	Ferritin light chain 1	Q6P7T1	6	21000	6,0	20981	7	53	3
40	Syntaxin-binding protein 3	Q60770	8,3	68000	6,0	64613	16	24	3
41	Synaptotagmin 5	Q56A28	9,4	43000	9,1	43084	8	20	1
42	AP-4 complex subunit sigma-1	Q9Y587	5,1	17000	3,7	18044	4	36	3
GTPase-related proteins									
43	Ras-related protein Rab-14	Q91V41	5,9	24000	6,0	23432	7	39	3
44	RAB15, member RAS oncogene family	Q504L6	5,4	24000	4,4	19298	6	29	1
45	Rho/Rac guanine nucleotide exchange fact	Q92974	8,7	101000	7,0	89066	6	8	3
Immune response									
46	MHC class I antigen	Q9MXM3	5,5	40000	5,9	30475	10	38	1
47	Lysozyme C	P61626	9,3	15000	8,5	18234	7	39	1
48	Cutaneous T-cell lymphoma-associated antigen	Q8IX95	4,9	18000	6,0	38747	5	48	2
49	Recombination-activating gene 1	Q5W9V9	6,4	38000	4,6	37876	11	41	2
50	Islet cell autoantigen 1-like protein	Q6RUG5	5,2	49000	5,4	59799	8	24	3
51	APG16 autophagy 16-like	Q3TDQ5	5,9	66000	7,0	61394	8	18	3
Extracellular matrix and related proteins									
52	Alpha-1 type I procollagen (fragment)	Q60785	5,7	35000	5,2	34660	11	42	1
53	Colla1 protein (fragment)	Q99LL6	5,9	59000	5,7	51246	7	20	1
53	Colla1 protein (fragment)	Q99LL6	5,9	59000	5,6	51626	12	30	1
54	Colla2 protein (fragment)	Q91VL4	7,1	57000	6,0	32431	7	15	1
55	procollagen, type III, alpha 1	Q8BJU6	5,9	36000	5,3	33602	10	36	1
56	Collagen alpha-1 (III) chain	P13941	9,4	94000	7,6	174792	15	20	1
57	Collagen alpha 1 (V) (fragment)	O70603	4,8	22000	4,4	36028	7	52	1
58	Glypican 1 variant (fragment)	Q59GI7	6,5	36000	5,6	33085	6	22	1
59	Perlecan	Q05793	5,9	17800	6,2	23432	8	11	1
Retinol-related proteins									
60	Dehydrogenase/reductase SDR family member	Q9BTZ2	7,7	28000	8,0	36876	4	11	3
61	Epididymal retinoic acid-binding protein	P06911	5,5	18000	5,3	23432	4	37	1

Secretion is indicated with (1) if the protein had a predicted signal peptide, (2) if it had a score >0,5 in neural network and therefore are nonclassically secreted, or (3) if they are not predicted as secreted. Proteins are listed with the accession number of Swiss-Prot and grouped in clusters of families and functions. (T) MW and pI as determined by UniProt database; (E) experimentally found in our 2D gels. % Cov: % of the sequence coverage by peptide mass fingerprinting using Aldente software, n.pep.: number of peptide masses matched.

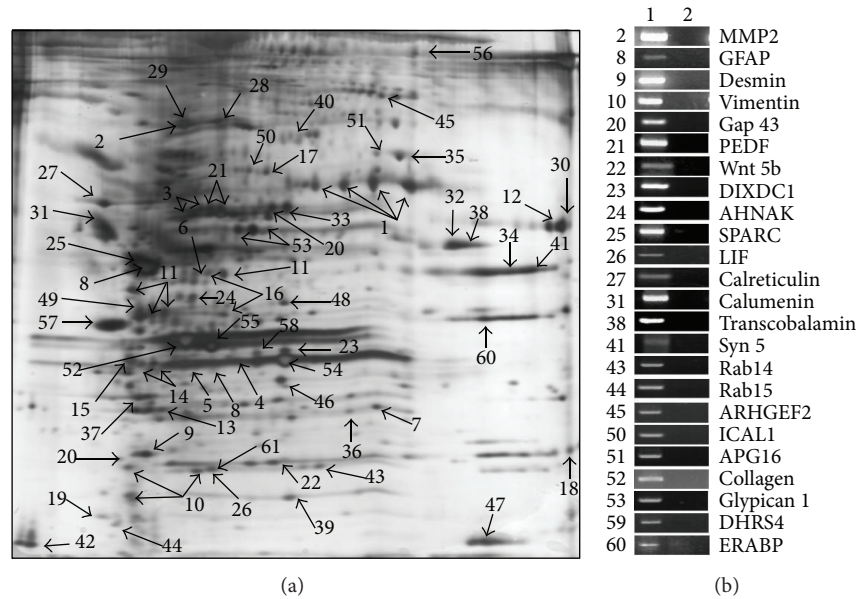


FIGURE 1: Secretome of PaSCs-ABCG2(+). (a) Silver-stained 2D gels of proteins secreted into the media by PaSCs-ABCG2(+). (b) Gene expression of some genes by RT-PCR, corresponding to the proteins identified by proteomic analysis. Total RNA from PaSCs-ABCG2(+) (lane 1), negative control (lane 2).

be secreted, either via classical pathways, that is, endoplasmic reticulum/Golgi-dependent pathway (contained a signal peptide), or via nonclassical pathways (without signal peptide, but with a Neural Network score superior than 0.5) (Table 2). The rest of the proteins were not predicted to be secreted by the current available software. However, we cannot exclude secretion via undescribed nonclassical mechanisms. Overall, we detected 37 soluble factors with a described secretion signature. Further analyses were performed by RT-PCR on a subset of candidate proteins in order to confirm the results obtained from proteomic analysis. For instance, we verified the identity of those factors relevant for their biological function and the ones that were identified as a gender different from rats. The proteins confirmed that the RNA levels are included in Figure 1(b). Among these proteins were some novel findings, including serpin family member PEDF, Wnt5b, and LIF. They were reported for the first time to be secreted by PaSC-ABCG2(+).

**3.3. Secretome Network Analysis.** To gain further insight into the potential functions of PaSC-ABCG2(+) secretome, we conducted proteomic data mining by Ingenuity Pathway Analysis 3.0 (Ingenuity Systems). Proteins identified in the secretome were submitted as “focus proteins” and were mapped onto the Ingenuity Pathways Knowledge Base, which is a database containing important curated information of interactions between genes, proteins, and other biological molecules. Our analysis rendered three main networks (Figures 2(a), 2(b), and 2(c)). Abbreviations of all the proteins used by the software are summarised in Table 3. The scores for all of the mapped networks were higher than 19, indicating that the networks selected were not due to random chance alone. These networks were associated with

the following functions: cellular assembly and organisation (network 1, score 27, 15 focused proteins), tissue development (network 2, score 27, 15 focus proteins), cell-to-cell signalling and interaction, and cellular growth and proliferation (network 3, score 22, 13 focus proteins). The first scored network (Figure 2(a)) highlighted TGF $\beta$ 1 as a nonfocused protein (included by the software to complete the network), which is located as a central node of the network.

The second and third scored networks obtained from Ingenuity Pathways are represented in Figures 2(b) and 2(c). Most of the factors implicated in development and differentiation processes are located in the extracellular compartment, with capacity to interact with the neighbouring cells. These soluble factors include SPARC, MMP2, PEDF, Wnt5b and collagens in the second network (Figure 2(b)), and LIF, which is also a secreted factor clustered in the third network (Figure 2(c)).

**3.4. TGF $\beta$ 1 Detection and Their Role in Cell Proliferation.** TGF $\beta$ 1 was a central protein highlighted in our secretome network (Figure 2(a)), and thus we decided to explore if this factor was present in our conditioned media. ELISA immunoassay of the conditioned media revealed that PaSC-ABCG2(+) secreted active TGF $\beta$ 1 at the concentration of  $48.95 \pm 5.18$  pg/mL ( $n = 10$ ) (Figure 3(a)). Our results were in agreement with previous reports [22, 23].

TGF $\beta$ 1 has a potent growth inhibitor capacity described in most cell types [24, 25] and is also capable of inducing Epithelial to Mesenchymal Transitions (EMT) in a variety of epithelial cells [26]. After detecting TGF $\beta$ 1 in the PaSC-ABCG2(+) conditioned media, we wanted to explore if this molecule had antiproliferative effects in ductal cell line (ARIP cells). In order to conduct these experiments, first we explore

TABLE 3: Abbreviations of all the proteins (focus and nonfocus) that appear in the three networks proposed by Ingenuity Pathways.

Name	Description	GenBank	Networks	Location	Family
AHNAK	AHNAK nucleoprotein (desmoyokin)	DQ203293	3	Nucleus	Other
AK2	Adenylate kinase 2	—	3	Cytoplasm	Kinase
ALDOA	Aldolase A, fructose-bisphosphate	M12919	3	Cytoplasm	Enzyme
ANXA4	Annexin A4	—	1	Plasma membrane	Other
ARHGEF2	rho/rac guanine nucleotide exchange factor (GEF) 2	NM_001012079	1	Cytoplasm	Other
BAT1	HLA-B associated transcript 1	—	1	Nucleus	Enzyme
CALR	Calreticulin	D78308	3	Nucleus	Transcription regulator
CALU	Calumenin	AJ001929	1	Unknown	Other
CBR1	Carbonyl reductase 1	X84349	3	Cytoplasm	Enzyme
CD300D	Cd300D antigen	—	3	Plasma membrane	Transmembrane receptor
CIAA1	CIA autoantibody QTL 1	—	2	Unknown	Other
CIAA2	CIA autoantibody QTL 2	—	2	Unknown	Other
CIB2	Calcium and integrin binding family member 2	—	3	Unknown	Kinase
CNN3	Calponin 3, acidic	—	1	Cytoplasm	Other
COL10A1	Collagen, type X, alpha 1	—	2	Extracellular space	Other
COL11A2	Collagen, type XI, alpha 2	—	2	Extracellular space	Other
COL14A1	Collagen, type XIV, alpha 1 (undulin)	—	2	Extracellular space	Other
COL1A1	Collagen, type I, alpha 1	XM_213440	2	Extracellular space	Other
COL1A2	Collagen, type I, alpha 2	AF121217	2	Extracellular space	Other
COL2A1	Collagen, type II, alpha 1	—	2	Extracellular space	Other
COL3A1	Collagen, type III, alpha 1	BC087039	2	Extracellular space	Other
COL5A1	Collagen, type V, alpha 1	AJ005394	1	Extracellular space	Other
COL5A3	Collagen, type V, alpha 3	—	2	Extracellular space	Other
CTSB	Cathepsin B	NM_022597	3	Cytoplasm	Peptidase
DDR1	Discoidin domain receptor family, member 1	—	2	Plasma membrane	Kinase
DDR2	Discoidin domain receptor family, member 2	—	2	Plasma membrane	Kinase
DDX18	DEAD (Asp-Glu-Ala-Asp) box polypeptide 18	—	1	Nucleus	Enzyme
DES	Desmin	NM_022531	1	Unknown	Other
DHRS4	Dehydrogenase/reductase (SDR family) member 4	NM_153315	1	Unknown	Enzyme
DIXDC1	DIX domain containing 1	NM_001037654	1	Unknown	Other
ELF3	E74-like factor 3	—	3	Nucleus	Transcription regulator
ENO1	Enolase 1, (alpha)	BC090069	1	Cytoplasm	Transcription regulator
F2	Coagulation factor II (thrombin)	—	3	Extracellular space	Peptidase
FCGR1B	Fc fragment of IgG, high affinity Ib, receptor (CD64)	—	3	Plasma membrane	Transmembrane receptor
FCGR1C	Fc fragment of IgG, high affinity Ic, receptor (CD64)	—	3	Plasma membrane	Transmembrane receptor
FFAR2	Free fatty acid receptor 2	—	3	Plasma membrane	G-protein coupled receptor
FOS	v-fos FBJ murine oncogene homolog	—	1	Nucleus	Transcription regulator

TABLE 3: Continued.

Name	Description	GenBank	Networks	Location	Family
FTL	Ferritin, light polypeptide	BC061525	3	Cytoplasm	Other
GAP43	Growth associated protein 43	NM_017195	2	Plasma membrane	Other
GFAP	Glial fibrillary acidic protein	U03700	3	Cytoplasm	Other
GSTA4	Glutathione s-transferase a4	—	3	Cytoplasm	Enzyme
HSPA5	Heat shock 70 kda protein 5	M14050	1	Cytoplasm	Other
HSPA8	Heat shock 70 kda protein 8	BC098914	2	Cytoplasm	Enzyme
HSPH1	Heat shock 105 kda/110 kda protein 1	—	2	Cytoplasm	Other
IL6	Interleukin 6 (interferon, $\beta$ 2)	—	3	Extracellular space	Cytokine
IL15	Interleukin 15	—	1	Extracellular space	Cytokine
IL1F6	Interleukin 1 family, member 6 (epsilon)	—	3	Extracellular space	Cytokine
IL1F9	Interleukin 1 family, member 9	—	3	Extracellular space	Cytokine
KCTD13	Potassium channel domain containing 13	—	3	Cytoplasm	Ion channel
KNG1	Kininogen 1	—	3	Extracellular space	Other
LARGE	Like-glycosyltransferase	—	3	Cytoplasm	Enzyme
LIF	Leukemia inhibitory factor	NM_022196	3	Extracellular space	Cytokine
LMNA	Lamin A/C	NM_001002016	2	Nucleus	Other
MAPK8	Mitogen-activated protein kinase 8	—	1	Cytoplasm	Kinase
MMP2	Matrix metalloproteinase 2	X71466	2	Extracellular Space	Peptidase
MYC	v-myc viral oncogene homolog	—	1	Nucleus	Transcription regulator
MYCN	v-myc viral related oncogene	—	3	Nucleus	Transcription regulator
MYL6	Myosin, light polypeptide 6	XM_001053789	3	Cytoplasm	Other
OMG	Oligodendrocyte myelin glycoprotein	—	1	Plasma membrane	G-protein coupled receptor
P4HA1	Procollagen-proline alpha polypeptide i	—	2	Cytoplasm	Enzyme
P4HB	Procollagen-proline, $\beta$ polypeptide	—	2	Cytoplasm	Enzyme
PCOLCE	Procollagen c-endopeptidase enhancer	U94710	2	Extracellular space	Other
PDLIM7	PDZ and LIM domain 7 (enigma)	—	1	Cytoplasm	Other
PGK1	Phosphoglycerate kinase 1	BC063161	1	Cytoplasm	Kinase
PKIG	Protein kinase inhibitor gamma	—	1	Unknown	Other
PKM2	Pyruvate kinase, muscle	M24359	3	Cytoplasm	Kinase
PLS3	Plastin 3 (t isoform)	—	1	Cytoplasm	Other
PLXNB2	Plexin b2	—	2	Plasma membrane	Other
PPP1R15A	Protein phosphatase 1, subunit 15a	—	2	Cytoplasm	Other
PRL	Prolactin	—	1	Extracellular space	Cytokine
PSMD6	Proteasome 26S subunit, non-ATPase, 6	NM_198730	1	Cytoplasm	Other
RAB14	RAB14, member RAS oncogene family	NM_053589	2	Cytoplasm	Enzyme
RAG1	Recombination activating gene 1	XM_001079242	3	Nucleus	Enzyme
RPS18	Ribosomal protein S18	—	1	Cytoplasm	Other
SERPINB8	Serpin peptidase inhibitor, clade B member 8	—	3	Cytoplasm	Other
SERPINE1	Serpin peptidase inhibitor, clade E member 1	—	2	Extracellular space	Other
SERPINF1	Serpin peptidase inhibitor, clade F (pigment epithelium derived factor)	BC078686	2	Extracellular space	Other

TABLE 3: Continued.

Name	Description	GenBank	Networks	Location	Family
SERPINH1	Serpin peptidase inhibitor, clade H (heat shock protein 47)	BC086529	2	Extracellular Space	Other
SLC16A5	Solute carrier family 16, member 5 (monocarboxylic acid transporter 6)	—	3	Plasma membrane	Transporter
SLCO1A2	Solute carrier organic anion transporter family, member 1A2	—	3	Plasma membrane	Transporter
SMARCB1	SWI/SNF related, matrix associated, subfamily b, member 1	—	2	Nucleus	Other
SP1	Sp1 transcription factor	—	3	Nucleus	Transcription regulator
SPARC	Secreted protein, acidic, cysteine-rich (osteonectin)	BC061777	2	Extracellular space	Other
STXBP3	Syntaxin binding protein 3	NM_053637	3	Plasma membrane	Transporter
SUMO2	SMT3 suppressor of mif two 3 homolog 2 (yeast)	—	1	Unknown	Other
TAGLN	Transgelin	NM_031549	3	Cytoplasm	Other
TCN2	Transcobalamin II, macrocytic anemia	AF054810	2	Extracellular space	Transporter
TGFB1	Transforming growth factor, $\beta$ 1	—	1	Extracellular space	Growth factor
THBS2	Thrombospondin 2	—	2	Extracellular space	Other
TNF	Tumor necrosis factor (TNF superfamily, member 2)	—	3	Extracellular space	Cytokine
TOR2A	Torsin family 2, member A	—	1	Extracellular space	Other
TP53	Tumor protein p53	—	2	Nucleus	Transcription regulator
TPM1	Tropomyosin 1 (alpha)	M60667	1	Cytoplasm	Other
TPM2	Tropomyosin 2 ( $\beta$ )	BC090009	1	Cytoplasm	Other
TPM3	Tropomyosin 3	NM_057208	1	Cytoplasm	Other
TPM4	Tropomyosin 4	J02780	1	Cytoplasm	Other
TSPAN7	Tetraspanin 7	—	1	Plasma membrane	Other
UBR2	Ubiquitin protein ligase E3 component n-recogin 2	—	3	Unknown	Enzyme
UPP1	Uridine phosphorylase 1	—	2	Cytoplasm	Enzyme
USP15	Ubiquitin specific peptidase 15	AF106657		Cytoplasm	Peptidase
VIM	Vimentin	X62952	2	Cytoplasm	Other
WNT5B	Wingless-type MMTV integration site family, member 5B	AF481944	2	Extracellular space	Other
YY2	YY2 transcription factor	—	1	Unknown	Other
ZBTB7B	Zinc finger and BTB domain containing 7B	—	2	Nucleus	Transcription regulator
ZFP161	Zinc finger protein 161 homolog (mouse)	—	1	Nucleus	Other

to see whether this cellular model has the capacity to respond to the TGF $\beta$ 1 signal. The analysis of TGF $\beta$  receptors (type I, type II, and type III) in ARIP cells showed that expression of these receptors when cells was cultured with basal medium or with PaSC-ABCG2(+) conditioned medium (Figure 3(b)).

**3.5. PaSC-ABCG2(+) Conditioned Media Inhibits Ductal Cell Proliferation without Altering Viability.** In order to evaluate the effects of the conditioned medium in ARIP cells, we

treated them during 24 hours and analysed the proliferation ratio by BrdU and their viability by MTT. The results showed that the rate of proliferation of ARIP cells treated with PaSC ABCG2(+) conditioned media was significantly reduced ( $40.3\% \pm 0.07$  relative to basal media no conditioned  $P < 0.01$ ,  $n = 4$ , Figure 4(a)). In order to test the specificity of conditioned media, we cultured ARIP cells with conditioned media collected from other cell lines, endocrine  $\alpha$ TC and ductal mPAC, and we found that proliferation rate was not modified (data not shown). In addition, ARIP cell

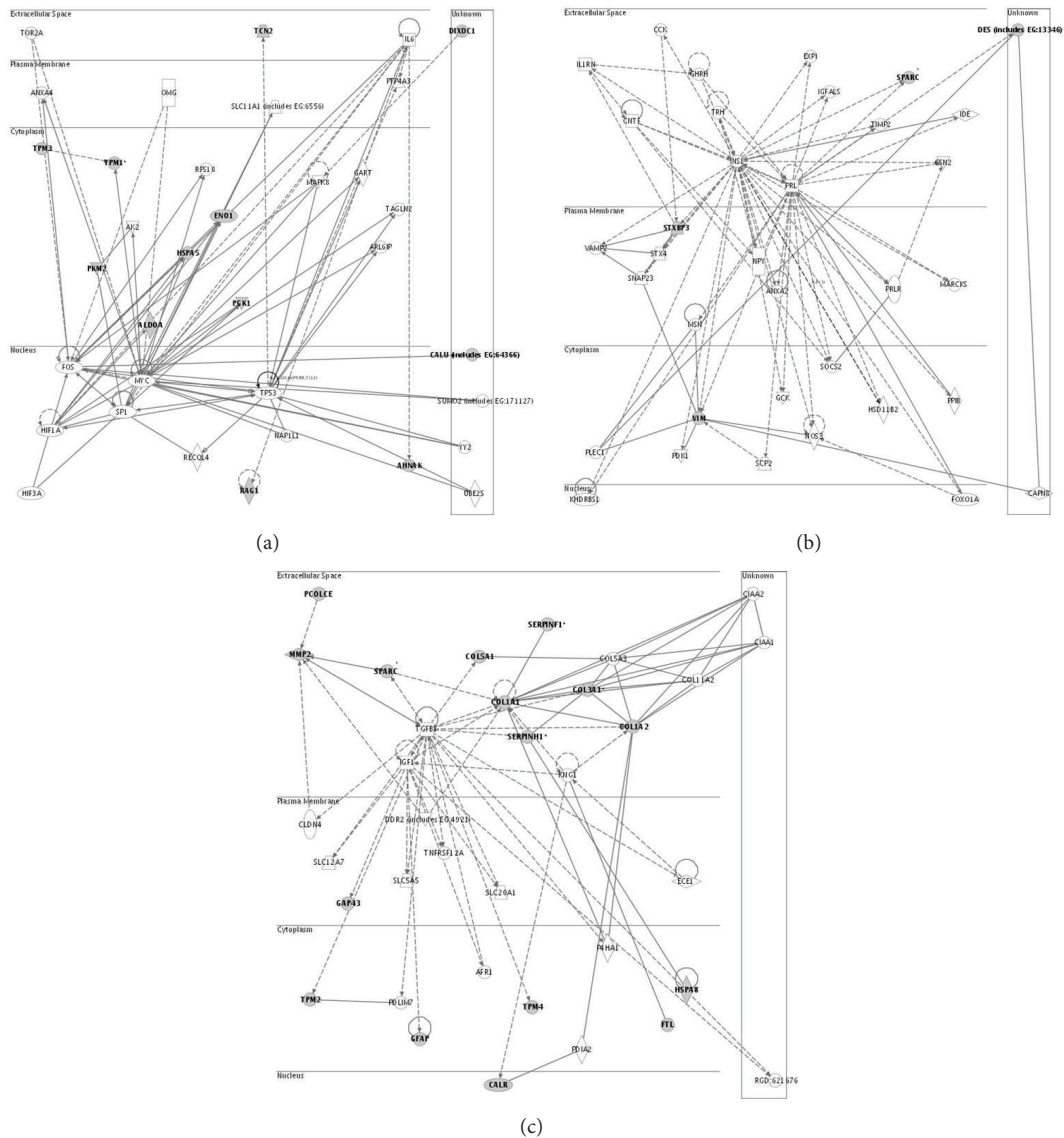


FIGURE 2: Ingenuity Pathways networks. These networks have resulted from submitting proteins identified in the secretome to the Ingenuity Pathways software. Proteins are classified in bold as focus proteins (which are obtained from our secretome results) or not in bold as nonfocus (which have been included by the software to complete the network). (a) The first network highlights  $TGF\beta 1$  as a “nonfocus” protein. (b) The second network includes novel proteins in the secretome of PaSC such as PEDF (SerpinF1) and Wnt5b, which have interactions with other soluble proteins in the extracellular space. (c) The third-scored network identifies LIF in the extracellular space. Legend of the node shapes to identify the type of protein: rhombus: enzyme, square: growth factor, inverted triangle: kinase, circle: other, rectangle: ion channel, oval: transcription regulator.

viability was not affected by PaSC-ABCG2(+) conditioned media (MTT test, data not shown). The conditioned media also significantly reduced proliferation in other cell lines used as controls: AR42J and MIN6 (data not shown). The results indicated that specific soluble factors secreted by these cells had effects on ARIP proliferation without altering cell viability. In order to check if  $TGF\beta 1$  was implicated in the antiproliferative effects of PaSC-ABCG2(+) secretome on ARIP cells, we blocked  $TGF\beta 1$  from the conditioned media with a pan  $TGF\beta$  antibody capable of neutralising its effects (Figure 3(c)). Adding pan-neutralising antibody to the conditioned media returned the rate of proliferation to

the basal level. As a positive control, we added exogenous  $TGF\beta 1$  (10 ng/mL) to the basal media, which significantly reduced the rate of proliferation ( $P < 0.05$ ), mimicking the effects of the stellate conditioned media. Exogenous  $TGF\beta 1$  can also be blocked by pan  $TGF\beta$  antibody, which returned the rate of proliferation to basal levels. Nonimmune IgG at 20  $\mu\text{g/mL}$  was used as control of exogenous antibody and its addition caused no modifications on the proliferation rate. Moreover, none of these treatments caused effects on cell viability, evaluated by MTT test (data not shown). These experiments confirmed the implication of  $TGF\beta 1$  secreted by stellate cells in the inhibition of the proliferation observed.

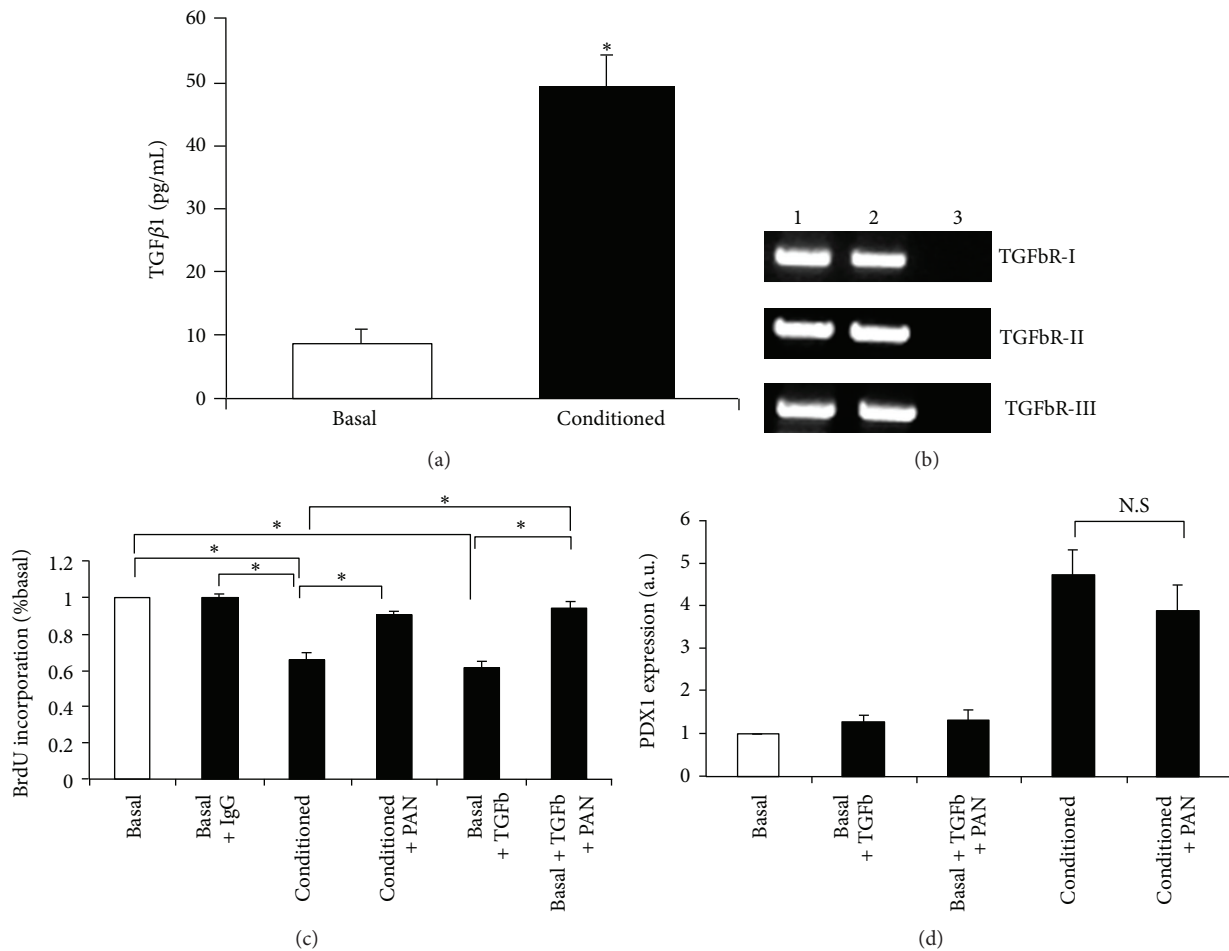


FIGURE 3: PaSCs-ABCG2(+) secrete TGFβ1, which causes the inhibition of proliferation but has no effect on PDX1 increase. (a) Quantification of active TGFβ1 in supernatant of PaSC cultured (conditioned media) for 24 hours. Active TGFβ1 was measured directly by ELISA, compared to TGFβ1 in the basal media ( $n = 8$ ). (b) Expression of TGFβ receptors in ARIP cells detected by RT-PCR. Lanes: 1-basal media, 2-conditioned media, 3-(-)RT. (c) Proliferation rate of ARIP cells (BrdU assay) after different stimulations: basal media, basal media plus nonimmune IgG 20 μg/mL, conditioned media, conditioned media plus Pan TGFβ 20 μg/mL, basal media plus TGFβ 10 ng/mL, or basal media plus pan TGFβ and TGFβ1. Results are expressed as percentage of control values (basal media) and are representative of 3 separate experiments. The neutralising antibody can revert the inhibition of proliferation in ARIP cells treated with conditioned media. \* indicate statistical significance with  $P < 0.05$ . (d) PDX1 expression of ARIP cells treated with basal media, conditioned media, conditioned media plus pan TGFβ 20 μg/mL, basal media plus TGFβ 10 ng/mL, or basal media plus pan TGFβ and TGFβ1. Results are expressed as fold increase of control values (basal media) and are representative of 6 independent experiments. NS indicates no statistical significance.

**3.6. PaSC-ABCG2(+) Conditioned Media Modify CK19 and PDX1 Expression on Ductal Cell Line.** Given the association between reducing cell proliferation and inducing differentiation, we decided to explore if PaSC-ABCG2(+) conditioned media produced changes in ARIP gene expression. The results showed that treatment with conditioned media during 72 hours caused a decrease of the ductal marker CK19, as detected by immunocytochemistry (Figure 4(b)). Quantitative real-time PCR indicated that conditioned media elicited a  $0.48 \pm 0.05$ -fold decrease in CK19 mRNA expression ( $n = 6$ ,  $P < 0.05$ , Figure 4(c)). These results indicate that PaSC-ABCG2(+) conditioned media are able to induce changes in transcription of endogenous ARIP gene CK19.

One of the most critical genes involved in endocrine differentiation and beta cell phenotype maintenance is the

transcription factor PDX1. In order to check if PaSC-ABCG2(+) conditioned media was able to modify PDX1 expression in this cellular model, first we evaluated the basal level of this transcription factor both at the protein and mRNA levels. We observed an increase of PDX1 when we treated them with PaSC-ABCG2(+) conditioned media (Figure 4(b)). Quantitative real-time PCR indicated that conditioned media treatment increased  $5.38$ -fold  $\pm 0.7$  PDX1 mRNA basal expression ( $n = 6$ ,  $P < 0.05$ , Figure 4(d)). To determine if TGFβ1 had a role in increasing PDX1 mRNA levels in ARIP cells treated with PaSC-ABCG2(+) conditioned media, we used the pan-neutralising TGFβ in the conditioned media during 72 hours. The blocking antibody did not reduce significantly PDX1 induction caused by the conditioned media. Moreover, the addition of exogenous

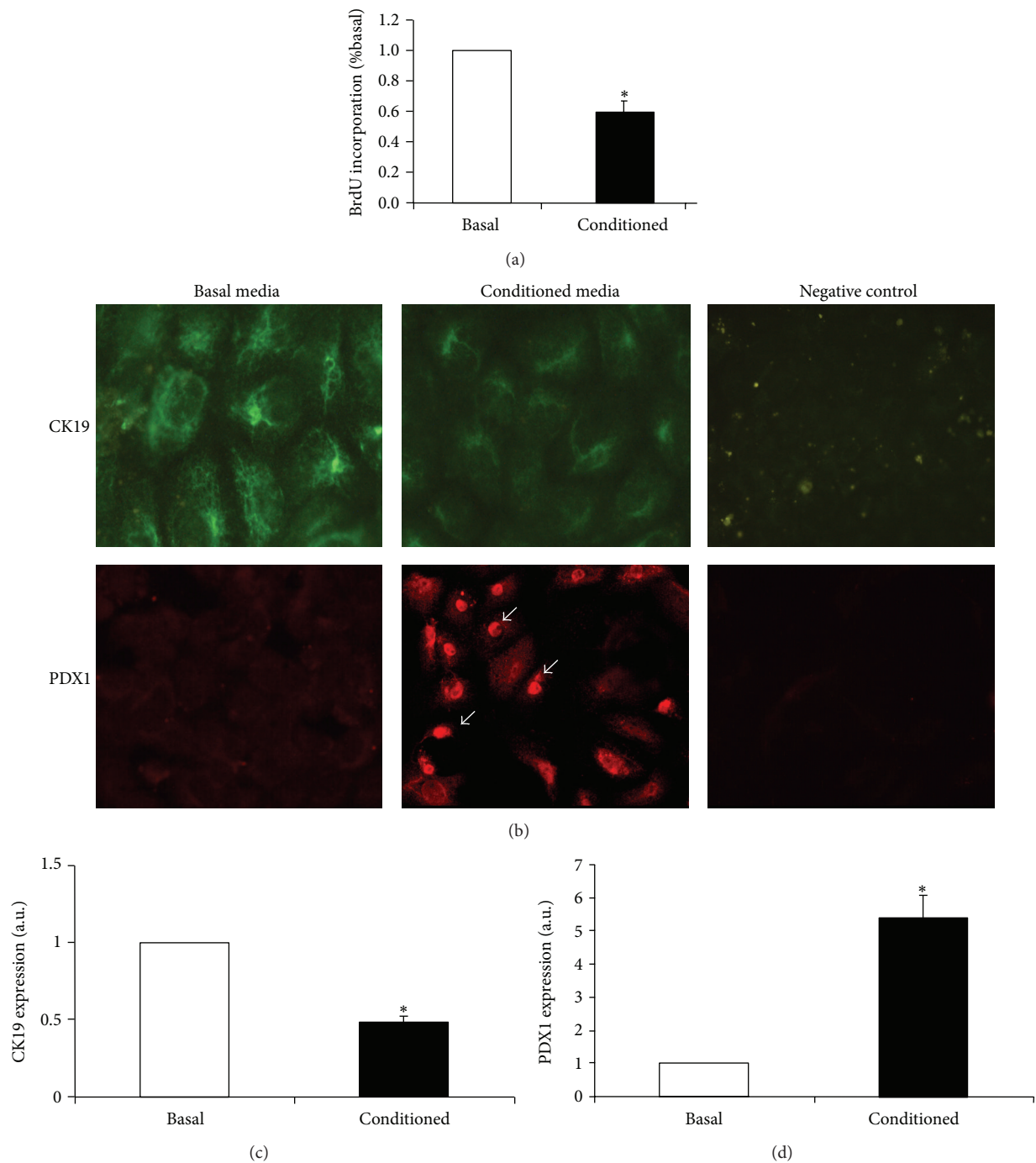


FIGURE 4: Conditioned media from PaSCs-ABCG2(+) inhibit proliferation and modify gene expression in the ARIP cell line. (a) Proliferation rate of ARIP cells (BrdU assay) after 24 hours of treatment with basal media and conditioned media from PaSCs-ABCG2(+). Results are expressed as percentage of control values (basal media) and are representative of 4 independent experiments. \* indicate statistical significance with  $P < 0.05$ . (b) Upper: immunocytochemistry of CK19 of ARIP cells treated for 72 hours with basal media (1) and conditioned media (2); only 2ari antibody (3). Magnification 20x. Lower: immunocytochemistry of PDX1 in ARIP cells treated for 72 hours basal media (1) and conditioned media (2); only 2ari antibody (3). Magnification 20x. ((c), (d)) CK19 and PDX1 expression by RT-PCR of ARIP cells treated for 72 hours with basal media (1) and conditioned media (2). mRNA levels present in cells treated with basal media were taken as reference and values were normalised to TBP mRNA levels. Bars indicate the SEM of three independent experiments performed in duplicate. \* indicate statistical significance with  $P < 0.05$ .

TGF $\beta$ 1 (10 ng/mL) to the control media for 72 hours did not induce PDX1 mRNA increased expression in ARIP cells (Figure 3(d)). These results indicate that TGF $\beta$ 1 is not apparently involved in PDX1 increased expression of ARIP-conditioned cells.

#### 4. Discussion

Hepatic stellate cells (HpSC) are morphologically and functionally similar to PaSC. Thus, most of the previous studies on stellate cells in the liver predict similar effects of stellate cells in the pancreas [27]. These two cell types have been compared at a transcriptional level, exhibiting organ-specific variations of a common transcriptional phenotype [27]. In the liver, activated stellate cells are known to influence the growth and proliferation of other liver cell types, particularly hepatocytes through paracrine effects [28, 29]. HpSC-derived Keratinocyte Growth Factor is thought to enhance liver regeneration and/or hepatocyte survival in patients with chronic liver disease [30]. Other reports indicate that coculture of HpSC with hepatocytes can preserve some aspects of hepatocyte function [31]. Stellate cells' effects on inducing differentiation have been described previously in liver; for instance, coculture of HpSC with stem cells gives rise to hepatocytes [32]. At present, there is no report of similar effects in the pancreas. Adult stem cells in the pancreas have not been localised yet, but there is some evidence of their ductal residence (transdifferentiation of ductal cells or remanent stem cells of the duct) [9, 33, 34]. Multiple secreted factors from PaSC, which are located in periacinar and periductal, could have a key contribution in maintaining the ductal niche. Our results indicate that soluble factors secreted by PaSC-ABCG2(+) can inhibit ductal proliferation, as they are also able of inducing changes of gene expression in ductal cells (decrease of the endogenous gene CK19 and increase of the endocrine transcription factor PDX1).

The proteomic approach using Ingenuity Pathway Analysis 3.0 conducted in PaSC-ABCG2(+) conditioned media predicted three main networks. One of them shed light on TGF $\beta$ 1 as a non-focused protein. This factor was not detected in 2D gels due to its low molecular weight (12 kDa), which was too small for the resolution of the gels used in the analysis. Alternatively, TGF $\beta$ 1 was detected by ELISA immunoassay. Using this technique, the results revealed that the levels of active TGF $\beta$ 1 secreted to the conditioned media are similar to the ones described by other primary cultures of PaSCs [22, 35]. It is known that the secretion of this protein is involved in the profibrogenic role of PaSC [36, 37]. Moreover, TGF $\beta$ 1 induces the transformation of PaSC to myofibroblasts (as evidenced by increased  $\alpha$ SMA expression) [38], and it also controls PaSC growth in an autocrine manner [39]. Our study demonstrated the capacity of the conditioned media obtained from PaSC culture to inhibit proliferation of the ARIP cell line and other cell lines, such as AR42J and MIN6, which were used as controls (data not shown). We identified TGF $\beta$ 1 as the main inhibitor of the ARIP proliferation.

Because cell proliferation arrest is generally accompanied by an increase in cell differentiation, we analysed ARIP gene expression. Our results demonstrated changes in CK19

and PDX1 on ARIP-conditioned cells; therefore we tried to identify the molecule involved in PDX1-increased expression (which is a transcription factor involved in endocrine differentiation). Our first goal was to explore TGF $\beta$ 1, based on previous studies that suggest a role of this factor in some differentiative processes [40, 41], including determination of pancreatic development [42, 43]. However, we were unable to demonstrate the role of TGF $\beta$ 1 on PDX1-enhanced expression in ARIP cells that have stopped proliferating, thus indicating that other soluble factors in the secretome had the capacity to modify PDX1 expression.

The second network also predicted by Ingenuity included *serpinf1* as a focus protein, also known as PEDE. This factor is involved in neurotrophic activity [44–46], and it has recently been involved in neural stem cell renewal as a niche signal [47]. It has been detected in the lung, the heart, and the liver, but its expression is nearly undetectable in the pancreas [48]. It was also interesting to find that this network also included a member of the Wingless family (Wnt5b). The WNT genes have been reported to play a pivotal role in embryonic development and oncogenesis; the isoform Wnt5b is expressed in the exocrine pancreas and upregulated in adipocyte differentiation [49, 50]. SPARC (secreted protein acidic and rich in cysteine), an extracellular Ca-binding glycoprotein associated with the morphogenesis and remodelling of various tissues [51], and MMP2 (matrix metalloproteinase-2), important metalloproteinase that has the capacity to activate TGF $\beta$ 1 [52], were also present as focus proteins in the second network. These proteins from our secretome (focus proteins) act as central nodes of the network, with described interactions between them.

Finally, the last network predicted highlights LIF, which has been described to induce astrocyte differentiation [53, 54] and is capable of generating insulin-producing beta cells from adult exocrine pancreatic cells in combination with EGF [55]. In this secretome we have found proteins associated with cell growth, development, and differentiation, which contain the novel findings PEDE, LIF, and Wnt5b. The data presented in our study provide a significant new protein-level insight into the secretome of active PaSCs-ABCG2(+). Some of these proteins may have potentially great influence on the physiology of the stellate cells themselves and/or of neighbouring cells. Further studies are required to determine a potential role of these factors in the PaSC-ABCG2(+) effects on ductal cells.

The type of secretion of the soluble factors analysed by SecretomeP indicated that 70% had a predicted signal peptide and 30% were secreted via nonclassical pathways which could involve membrane blebbing, exosomes, plasma membrane resident transporters, or lysosomal secretion [56]. Any of the secreted factors could be the potential candidates to exert the effects of the PaSC-ABCG2(+) conditioned media. The most abundant family of secreted factors is the extracellular matrix and related proteins, which coincides with the main function of PaSC (remodelling extracellular matrix remodeling and turnover). This family includes perlecan and collagens, components of the extracellular matrix which contribute to the creation of a microenvironment around PaSC acting as a pool of cytokines and growth factors. It should be noted that not all

the proteins identified in our study are known to be secreted. The ones, which have no evidence of secretion, may originate from the minority of cells that die or are otherwise disrupted during the washing and harvesting steps of the procedure and also possibly secreted by unknown mechanisms. This is a common issue in proteomic analysis performed on secretome from primary cell cultures. Most of these proteins were derived from the intracellular compartment characteristic of the stellate phenotype and should be useful for their characterisation. Moreover, some of the proteins identified in the secretome were previously described to be secreted by hepatic stellate cells, such as SPARC, MMP2, cathepsin B, and collagens. The structural ones (calreticulin,  $\alpha$ -enolase, and vimentin) were also present in the study of hepatic stellate cells [56], and they were confirmed as the stellate phenotype in our study.

In summary, we have described new soluble factors secreted by PaSC-ABCG2(+) cell population. The characterization of this secretome opens a new field of research involved in paracrine actions, such as inhibition of the proliferation and differentiation promotion in the ductal cell model.

## List of Abbreviations

PaSC-ABCG2(+):	Pancreatic stellate cells
HpSC:	Hepatic stellate cells
RT-PCR:	Reverse transcriptase-polymerase chain reaction
BrdU:	Bromodeoxyuridine
MTT:	3-(4,5-Dimethylthiazol-2-yl)-2,5-diphenyl-2H-tetrazolium bromide
BSA:	Bovine serum albumin
FCS:	Foetal calf serum
TGF $\beta$ :	Transforming growth factor $\beta$
PSA-NCAM:	Polysialic acid-neural cell adhesion molecule
MALDI-TOF:	Matrix assisted laser desorption/ionization-time of flight
2D:	Two-dimensional electrophoresis.

## Conflict of Interests

The authors declare that they have no conflict of interests.

## Authors' Contribution

Maria Lucas and Eugenia Mato contributed equally to this paper.

## Acknowledgments

The authors thank Scientific and Technical Services of the Institute of Biomedical Research August Pi i Sunyer (IDIBAPS): Isabel Crespo (Flow Cytometry Unit) and Dr. Susana Kalko (Bioinformatics Unit). The authors thank Dr. Josep M Estanyol for MS analyses from the Proteomic Unit of SSR University of Barcelona and Dr. Eliandre Oliveira from

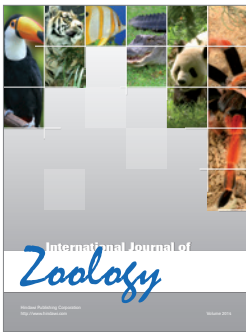
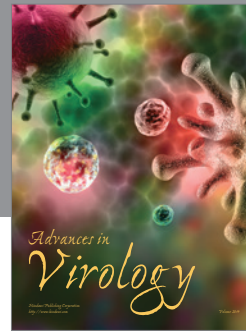
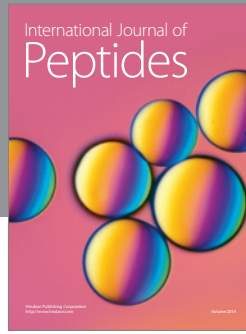
Proteomics Unit of Parc Científic de Barcelona for MALDI-TOF and MS/MS spectra acquisition. Proteomic Units are members of Spanish ProteoRed. They also would like to thank Yaiza Esteban for technical assistance in proteomics studies. This project was funded by grants from SAF2006-07382, RGDMG03/212, PI042553, PI020881, and RETIC RD06/0015/0002 and supported by Sardà Farriol Research Program. CIBER de Diabetes y Enfermedades Metabólicas Asociadas is an ISCIII project.

## References

- [1] M. V. Apte, P. S. Haber, S. J. Darby et al., "Pancreatic stellate cells are activated by proinflammatory cytokines: implications for pancreatic fibrogenesis," *Gut*, vol. 44, no. 4, pp. 534–541, 1999.
- [2] M. B. Omary, A. Lugea, A. W. Lowe, and S. J. Pandol, "The pancreatic stellate cell: a star on the rise in pancreatic diseases," *Journal of Clinical Investigation*, vol. 117, no. 1, pp. 50–59, 2007.
- [3] T. Knittel, S. Aurisch, K. Neubauer, S. Eichhorst, and G. Ramadori, "Cell-type-specific expression of neural cell adhesion molecule (N-CAM) in Ito cells of rat liver: up-regulation during in vitro activation and in hepatic tissue repair," *American Journal of Pathology*, vol. 149, no. 2, pp. 449–462, 1996.
- [4] R. A. Hannivoort, S. Dunning, S. V. Borghet et al., "Multidrug resistance-associated proteins are crucial for the viability of activated rat hepatic stellate cells," *Hepatology*, vol. 48, no. 2, pp. 624–634, 2008.
- [5] E. Schneider, A. Schmid-Kotsas, J. Zhao et al., "Identification of mediators stimulating proliferation and matrix synthesis of rat pancreatic stellate cells," *American Journal of Physiology—Cell Physiology*, vol. 281, no. 2, pp. C532–C543, 2001.
- [6] K. Shimizu, M. Kobayashi, J. Tahara, and K. Shiratori, "Cytokines and peroxisome proliferator-activated receptor  $\gamma$  ligand regulate phagocytosis by pancreatic stellate cells," *Gastroenterology*, vol. 128, no. 7, pp. 2105–2118, 2005.
- [7] P. A. Phillips, J. A. McCarroll, S. Park et al., "Rat pancreatic stellate cells secrete matrix metalloproteinases: implications for extracellular matrix turnover," *Gut*, vol. 52, no. 2, pp. 275–282, 2003.
- [8] X. Xu, J. D'Hoker, G. Stangé et al., " $\beta$  cells can be generated from endogenous progenitors in injured adult mouse pancreas," *Cell*, vol. 132, no. 2, pp. 197–207, 2008.
- [9] S. Bonner-Weir, E. Toschi, A. Inada et al., "The pancreatic ductal epithelium serves as a potential pool of progenitor cells," *Pediatric Diabetes*, vol. 5, supplement 2, pp. 16–22, 2004.
- [10] S. Bonner-Weir, M. Taneja, G. C. Weir et al., "In vitro cultivation of human islets from expanded ductal tissue," *Proceedings of the National Academy of Sciences of the United States of America*, vol. 97, no. 14, pp. 7999–8004, 2000.
- [11] L. Bouwens and D. G. Pipeleers, "Extra-insular beta cells associated with ductules are frequent in adult human pancreas," *Diabetologia*, vol. 41, no. 6, pp. 629–633, 1998.
- [12] E. Mato, M. Lucas, J. Petriz, R. Gomis, and A. Novials, "Identification of a pancreatic stellate cell population with properties of progenitor cells: new role for stellate cells in the pancreas," *Biochemical Journal*, vol. 421, no. 2, pp. 181–191, 2009.
- [13] U. Rutishauser and L. Landmesser, "Polysialic acid in the vertebrate nervous system: a promoter of plasticity in cell-cell interactions," *Trends in Neurosciences*, vol. 19, no. 10, pp. 422–427, 1996.

- [14] T. Ben-Hur, B. Register, K. Murray, G. Rougon, and M. Dubois-Dalcq, "Growth and fate of PSA-NCAM+ precursors of the postnatal brain," *Journal of Neuroscience*, vol. 18, no. 15, pp. 5777–5788, 1998.
- [15] S. Barcelo-Batllori, H. Corominola, M. Claret, I. Canals, J. Guinovart, and R. Gomis, "Target identification of the novel antiobesity agent tungstate in adipose tissue from obese rats," *Proteomics*, vol. 5, no. 18, pp. 4927–4935, 2005.
- [16] A. Shevchenko, M. Wilm, O. Vorm, and M. Mann, "Mass spectrometric sequencing of proteins from silver-stained polyacrylamide gels," *Analytical Chemistry*, vol. 68, no. 5, pp. 850–858, 1996.
- [17] S. Barcelo-Batllori, M. Andre, C. Servis et al., "Proteomic analysis of cytokine induced proteins in human intestinal epithelial cells: implications for inflammatory bowel diseases," *Proteomics*, vol. 2, pp. 551–560, 2002.
- [18] S. Barceló-Batllori, S. G. Kalko, Y. Esteban, S. Moreno, M. C. Carmona, and R. Gomis, "Integration of DIGE and bioinformatics analyses reveals a role of the antiobesity agent tungstate in redox and energy homeostasis pathways in brown adipose tissue," *Molecular and Cellular Proteomics*, vol. 7, no. 2, pp. 378–393, 2008.
- [19] J. D. Bendtsen, L. J. Jensen, N. Blom, G. von Heijne, and S. Brunak, "Feature-based prediction of non-classical and leaderless protein secretion," *Protein Engineering, Design and Selection*, vol. 17, no. 4, pp. 349–356, 2004.
- [20] O. Emanuelsson, S. Brunak, G. von Heijne, and H. Nielsen, "Locating proteins in the cell using TargetP, SignalP and related tools," *Nature Protocols*, vol. 2, no. 4, pp. 953–971, 2007.
- [21] G. Alvarez-Llamas, E. Szalowska, M. P. de Vries et al., "Characterization of the human visceral adipose tissue secretome," *Molecular and Cellular Proteomics*, vol. 6, no. 4, pp. 589–600, 2007.
- [22] F. W.-T. Shek, R. C. Benyon, F. M. Walker et al., "Expression of transforming growth factor- $\beta$ 1 by pancreatic stellate cells and its implications for matrix secretion and turnover in chronic pancreatitis," *American Journal of Pathology*, vol. 160, no. 5, pp. 1787–1798, 2002.
- [23] H. Ohnishi, T. Miyata, H. Yasuda et al., "Distinct roles of smad2-, smad3-, and ERK-dependent pathways in transforming growth factor- $\beta$ 1 regulation of pancreatic stellate cellular functions," *Journal of Biological Chemistry*, vol. 279, no. 10, pp. 8873–8878, 2004.
- [24] J. Massague, S. Cheifetz, M. Laiho, D. A. Ralph, F. M. B. Weis, and A. Zentella, "Transforming growth factor- $\beta$ ," *Cancer Surveys*, vol. 12, pp. 81–103, 1992.
- [25] S. S. Huang and J. S. Huang, "TGF- $\beta$  control of cell proliferation," *Journal of Cellular Biochemistry*, vol. 96, no. 3, pp. 447–462, 2005.
- [26] M. Kondo, E. Cubillo, K. Tobiume et al., "A role for Id in the regulation of TGF- $\beta$ -induced epithelial-mesenchymal transdifferentiation," *Cell Death and Differentiation*, vol. 11, no. 10, pp. 1092–1101, 2004.
- [27] M. Buchholz, H. A. Kestler, K. Holzmann et al., "Transcriptome analysis of human hepatic and pancreatic stellate cells: organ-specific variations of a common transcriptional phenotype," *Journal of Molecular Medicine*, vol. 83, no. 10, pp. 795–805, 2005.
- [28] A. M. Gressner, "The cell biology of liver fibrogenesis—an imbalance of proliferation, growth arrest and apoptosis of myofibroblasts," *Cell and Tissue Research*, vol. 292, no. 3, pp. 447–452, 1998.
- [29] H. Steiling, M. Muhlbauer, F. Bataille, J. Schölmerich, S. Werner, and C. Hellerbrand, "Activated hepatic stellate cells express keratinocyte growth factor in chronic liver disease," *The American Journal of Pathology*, vol. 165, pp. 1233–1241, 2004.
- [30] R. J. Thomas, R. Bhandari, D. A. Barrett et al., "The effect of three-dimensional co-culture of hepatocytes and hepatic stellate cells on key hepatocyte functions in vitro," *Cells Tissues Organs*, vol. 181, no. 2, pp. 67–79, 2006.
- [31] H. Nagai, K. Terada, G. Watanabe et al., "Differentiation of liver epithelial (stem-like) cells into hepatocytes induced by coculture with hepatic stellate cells," *Biochemical and Biophysical Research Communications*, vol. 293, no. 5, pp. 1420–1425, 2002.
- [32] X. Xu, J. D'Hoker, G. Stangé et al., " $\beta$  cells can be generated from endogenous progenitors in injured adult mouse pancreas," *Cell*, vol. 132, no. 2, pp. 197–207, 2008.
- [33] S. Yatoh, R. Dodge, T. Akashi et al., "Differentiation of affinity-purified human pancreatic duct cells to  $\beta$ -cells," *Diabetes*, vol. 56, no. 7, pp. 1802–1809, 2007.
- [34] H. Aoki, H. Ohnishi, K. Hama et al., "Existence of autocrine loop between interleukin-6 and transforming growth factor- $\beta$ 1 in activated rat pancreatic stellate cells," *Journal of Cellular Biochemistry*, vol. 99, no. 1, pp. 221–228, 2006.
- [35] S. G. Rane, J.-H. Lee, and H.-M. Lin, "Transforming growth factor- $\beta$  pathway: role in pancreas development and pancreatic disease," *Cytokine and Growth Factor Reviews*, vol. 17, no. 1-2, pp. 107–119, 2006.
- [36] C. Kordes, S. Brookmann, D. Häussinger, and H. Klonowski-Stumpe, "Differential and synergistic effects of platelet-derived growth factor-BB and transforming growth factor- $\beta$ 1 on activated pancreatic stellate cells," *Pancreas*, vol. 31, no. 2, pp. 156–167, 2005.
- [37] M. V. Apte, P. S. Haber, T. L. Applegate et al., "Periacinar stellate shaped cells in rat pancreas: identification, isolation, and culture," *Gut*, vol. 43, no. 1, pp. 128–133, 1998.
- [38] M.-L. Kruse, P. B. Hildebrand, C. Timke, U. R. Fölsch, and W. E. Schmidt, "TGF $\beta$ 1 autocrine growth control in isolated pancreatic fibroblastoid cells/stellate cells in vitro," *Regulatory Peptides*, vol. 90, no. 1–3, pp. 47–52, 2000.
- [39] C. Zhu, D. Ying, D. Zhou et al., "Expression of TGF- $\beta$ 1 in smooth muscle cells regulates endothelial progenitor cells migration and differentiation," *Journal of Surgical Research*, vol. 125, no. 2, pp. 151–156, 2005.
- [40] F. Han, C. S. Adams, Z. Tao et al., "Transforming growth factor- $\beta$ 1 (TGF- $\beta$ 1) regulates ATDC5 chondrogenic differentiation and fibronectin isoform expression," *Journal of Cellular Biochemistry*, vol. 95, no. 4, pp. 750–762, 2005.
- [41] F. Sanvito, P.-L. Herrera, J. Huarte et al., "TGF- $\beta$ 1 influences the relative development of the exocrine and endocrine pancreas in vitro," *Development*, vol. 120, no. 12, pp. 3451–3462, 1994.
- [42] E. Tei, S. Mehta, S. S. Tulachan et al., "Synergistic endocrine induction by GLP-1 and TGF- $\beta$  in the developing pancreas," *Pancreas*, vol. 31, no. 2, pp. 138–141, 2005.
- [43] S. P. Becerra, "Structure-function studies on PEDF: a noninhibitory serpin with neurotrophic activity," *Advances in Experimental Medicine and Biology*, vol. 425, pp. 223–237, 1997.
- [44] J. Tombran-Tink, G. G. Chader, and L. V. Johnson, "PEDF: a pigment epithelium-derived factor with potent neuronal differentiative activity," *Experimental Eye Research*, vol. 53, no. 3, pp. 411–414, 1991.

- [45] F. R. Steele, G. J. Chader, L. V. Johnson, and J. Tombran-Tink, "Pigment epithelium-derived factor: neurotrophic activity and identification as a member of the serine protease inhibitor gene family," *Proceedings of the National Academy of Sciences of the United States of America*, vol. 90, no. 4, pp. 1526–1530, 1993.
- [46] C. Ramírez-Castillejo, F. Sánchez-Sánchez, C. Andreu-Agulló et al., "Pigment epithelium-derived factor is a niche signal for neural stem cell renewal," *Nature Neuroscience*, vol. 9, no. 3, pp. 331–339, 2006.
- [47] J. Tombran-Tink, K. Mazuruk, I. R. Rodriguez et al., "Organization, evolutionary conservation, expression and unusual Alu density of the human gene for pigment epithelium-derived factor, a unique neurotrophic serpin," *Molecular Vision*, vol. 2, p. 11, 1996.
- [48] R. S. Heller, T. Klein, Z. Ling et al., "Expression of Wnt, frizzled, sFRP, and DKK genes in adult human pancreas," *Gene Expression*, vol. 11, no. 3-4, pp. 141–147, 2003.
- [49] A. Kanazawa, S. Tsukada, A. Sekine et al., "Association of the gene encoding wingless-type mammary tumor virus integration-site family member 5B (WNT5B) with type 2 diabetes," *American Journal of Human Genetics*, vol. 75, no. 5, pp. 832–843, 2004.
- [50] W. J. Cho, E. J. Kim, S. J. Lee, H. D. Kim, H. J. Shin, and W. K. Lim, "Involvement of SPARC in in vitro differentiation of skeletal myoblasts," *Biochemical and Biophysical Research Communications*, vol. 271, no. 3, pp. 630–634, 2000.
- [51] J. D. Mott and Z. Werb, "Regulation of matrix biology by matrix metalloproteinases," *Current Opinion in Cell Biology*, vol. 16, no. 5, pp. 558–564, 2004.
- [52] L. Bugga, R. A. Gadiant, K. Kwan, C. L. Stewart, and P. H. Patterson, "Analysis of neuronal and glial phenotypes in brains of mice deficient in leukemia inhibitory factor," *Journal of Neurobiology*, vol. 36, pp. 509–524, 1998.
- [53] M. Nakanishi, T. Niidome, S. Matsuda, A. Akaike, T. Kihara, and H. Sugimoto, "Microglia-derived interleukin-6 and leukaemia inhibitory factor promote astrocytic differentiation of neural stem/progenitor cells," *European Journal of Neuroscience*, vol. 25, no. 3, pp. 649–658, 2007.
- [54] L. Baeyens, S. de Breuck, J. Lardon, J. K. Mfopou, I. Rooman, and L. Bouwens, "In vitro generation of insulin-producing beta cells from adult exocrine pancreatic cells," *Diabetologia*, vol. 48, no. 1, pp. 49–57, 2005.
- [55] W. Nickel, "Unconventional secretory routes: direct protein export across the plasma membrane of mammalian cells," *Traffic*, vol. 6, no. 8, pp. 607–614, 2005.
- [56] D. Bach Kristensen, N. Kawada, K. Imamura et al., "Proteome analysis of rat hepatic stellate cells," *Hepatology*, vol. 32, no. 2, pp. 268–277, 2000.



**Hindawi**

Submit your manuscripts at  
<http://www.hindawi.com>

